SUPPLEMENTARY INFORMATION

Type I interferon signaling induces melanoma cell-intrinsic PD-1 and its inhibition antagonizes immune checkpoint blockade

Julia Holzgruber[1,2,3,4,+], Christina Martins[1,2,3,+], Zsofi Kulcsar[1,2,3,5,+], Alexandra Duplaine[1,6], Erik Rasbach[1,2,3,7], Laure Migayron[1,2,3], Praveen Singh[1,2,3], Edith Statham[1,2], Jennifer Landsberg[5], Katia Boniface[8], Julien Seneschal[6,8], Wolfram Hoetzenecker[4], Emma L. Berdan[9], Shannan Ho Sui[9], Matthew R. Ramsey[1,2], Steven R. Barthel[1,2,3,*], Tobias Schatton[1,2,3,10,*]

***Authors for correspondence:**

Tobias Schatton, Email: tschatton@bwh.harvard.edu

Steven R. Barthel, Email: sbarthel@bwh.harvard.edu

This PDF file includes:

Supplementary Figures 1-16

Supplementary Tables 1-4

Supplementary Figures

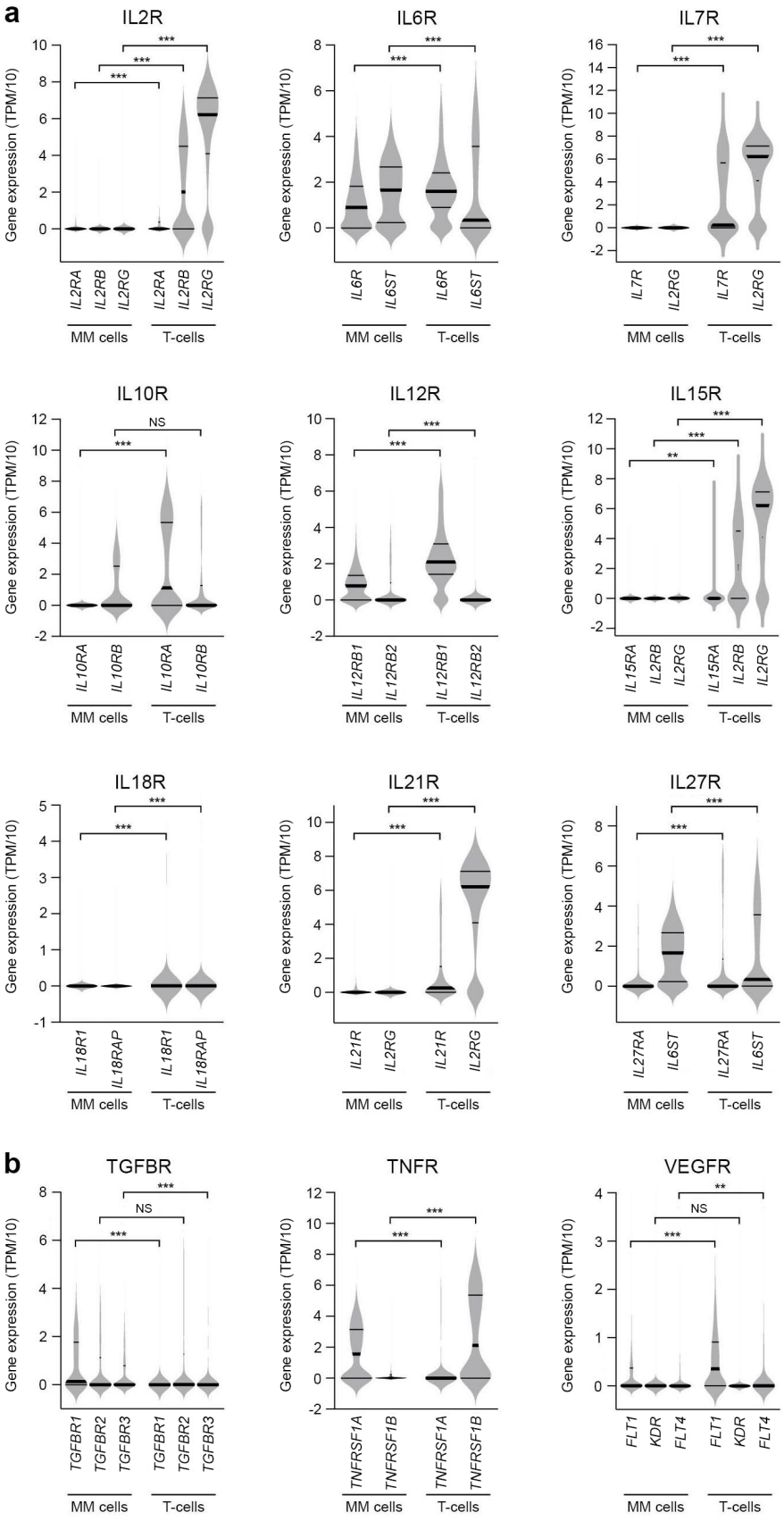

Supplementary Figure 1. Expression of cytokine and growth factor receptors by patient melanoma cells. Related to Figure 1. Single-cell RNA-seq analysis of **a,** cytokine receptor and **b,** growth factor receptor gene expression in patient melanoma (MM) versus tumor-infiltrating T-cells. Violin plots depict respective receptor subunit expression (median, bold black line; top and bottom quartiles, thin black lines). Results represent biologically independent samples of (**a**-**b**) n = 1252 MM cells and n = 2040 T-cells. Statistical analyses in (**a**-**b**) included the Mann-Whitney test, two-sided. **, $p < 0.01$; ***, $p < 0.001$; NS, not significant. Source data, including exact p-values, are provided as a Source Data file.

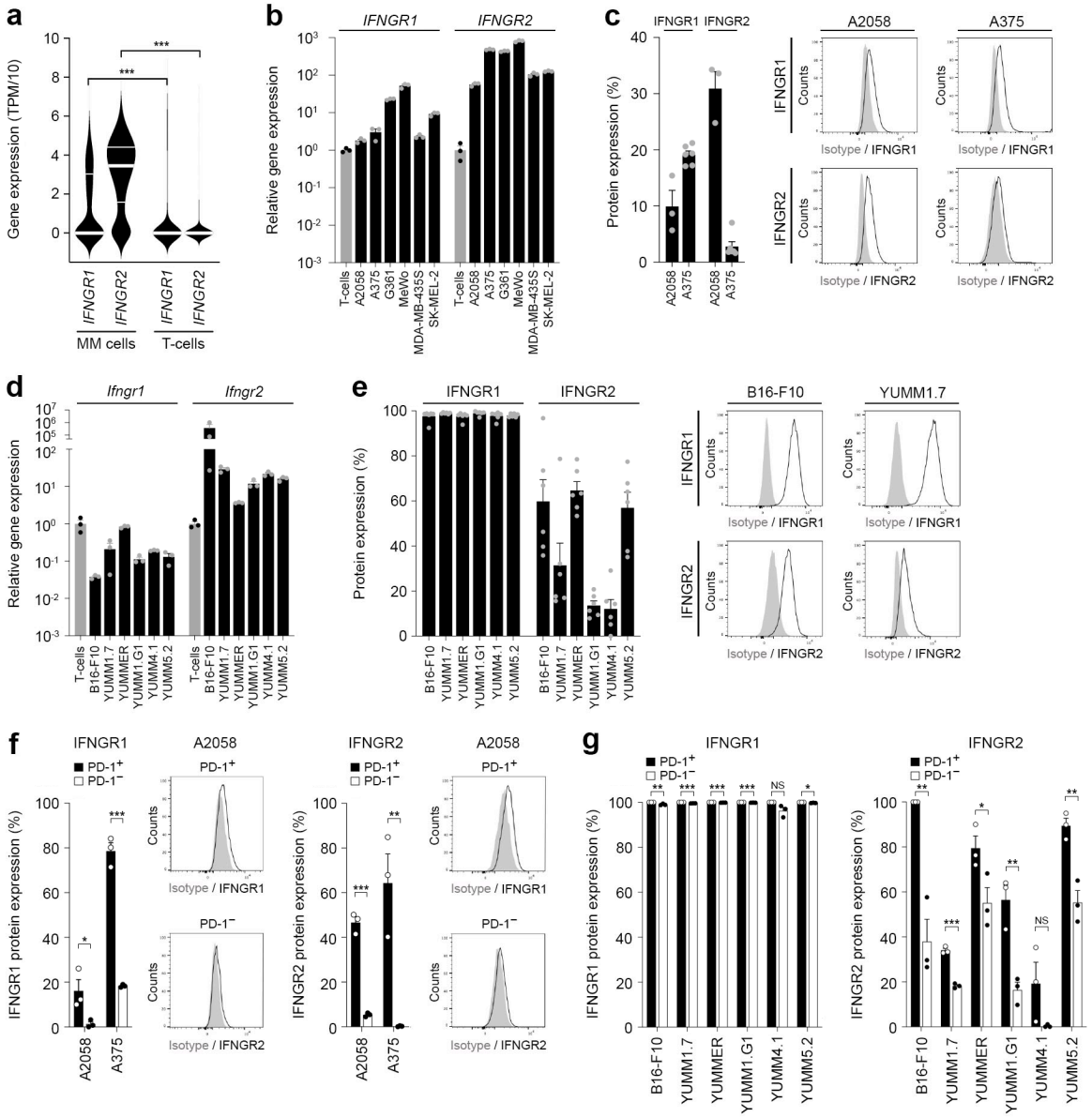

Supplementary Figure 2. Expression of the interferon-gamma receptor by melanoma cells. Related to Figure 1. Single-cell RNA-seq analysis of **a,** type II interferon-γ receptor (IFNGR) subunit gene expression in patient melanoma (MM) cells (left) versus tumor-infiltrating T-cells (right) as depicted by violin plots (median, bold white line; top and bottom quartiles, thin white lines) **b,** Relative *IFNGR1* and *IFNGR2* gene expression (fold change, mean ± SEM) in human melanoma cell lines (black bars) versus human T-cells (gray bars) as determined by RT-qPCR. **c,** IFNGR1 and IFNGR2 surface protein expression (percent positivity, mean ± SEM, left) by human A2058 and A375 melanoma cells, with representative flow cytometric histograms shown (right). **d,** Relative *Ifngr1* and *Ifngr2* gene expression (fold change, mean ± SEM) in murine melanoma cell lines (black bars) versus murine T-cells (gray bars) as determined by RT-qPCR. **e,** IFNGR1 and IFNGR2 surface protein expression (percent positivity, mean ± SEM, left) by murine

melanoma cells, with representative flow cytometric histograms shown for B16-F10 and YUMM1.7 melanoma cells (right). **f-g,** IFNGR1 (left) and IFNGR2 (right) surface protein expression (percent positivity, mean ± SEM) by PD-1^{+} versus PD-1^{-} **f,** human A2058 and **g,** murine melanoma cell subsets, with representative flow cytometric histograms shown for A2058 cells. Results represent biologically independent samples of (**a**) n = 1252 MM cells and n = 2040 T-cells, and biologically independent experiments of (**b**,**d**,**f**,**g**) n = 3, (**c**) n = 3 (A2058), n = 6 (A375), and (**e**) n = 6. Statistical analyses included the (**a**) Mann-Whitney test, two-sided and (**f-g**) unpaired t-test, two-sided. *, $p < 0.05$; **, $p < 0.01$; ***, $p < 0.001$; NS, not significant. Source data, including exact p-values, are provided as a Source Data file.

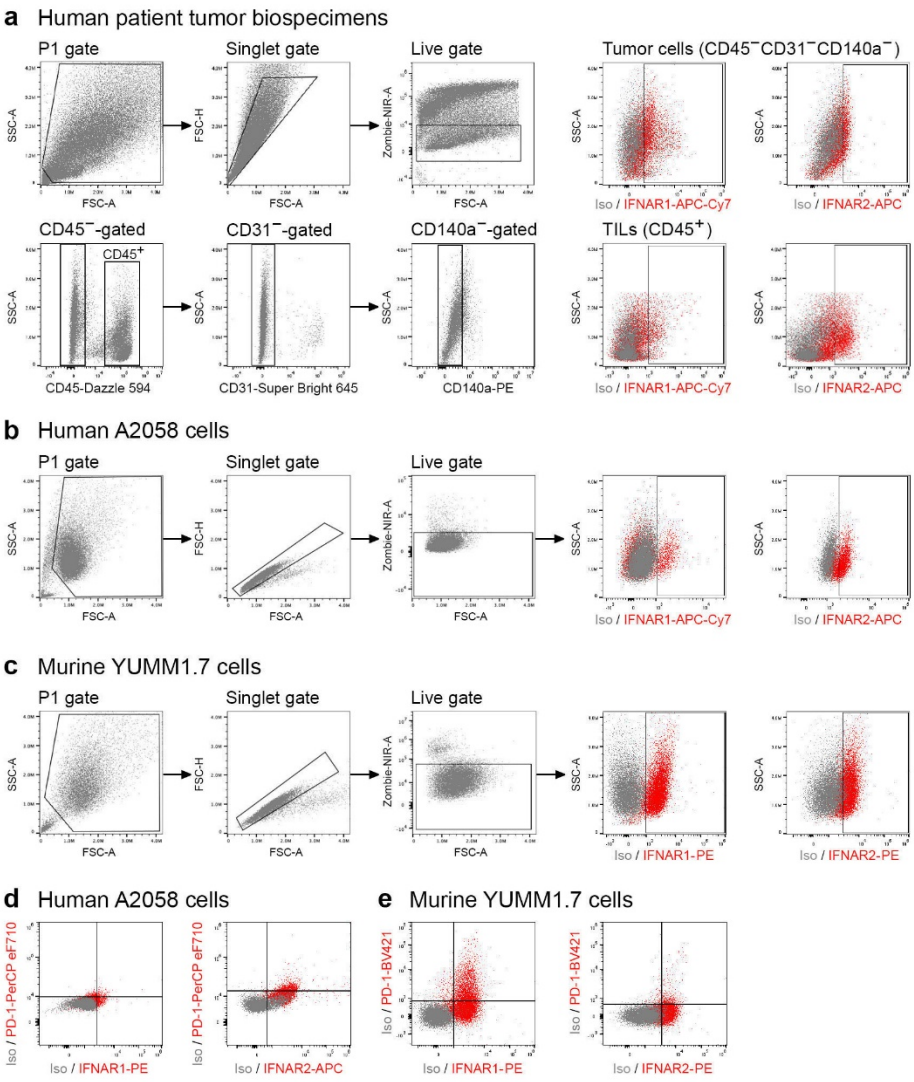

Supplementary Figure 3. Flow cytometry gating strategies for analysis of type I interferon receptor and PD-1 surface protein expression by patient tumor cells or melanoma lines. Related to Figure 1. Flow cytometry gating strategies and representative dot plots for IFNAR1 (left) or IFNAR2 (right) surface protein expression by **a,** human patient tumor cells (top) and tumor-infiltrating lymphocytes (TILs, bottom), **b,** human A2058 melanoma cells, and **c,** murine YUMM1.7 melanoma cells. **d-e,** Representative dot plots of IFNAR1 or IFNAR2 co-expression with PD-1 on **d,** human A2058 and **e,** murine YUMM1.7 melanoma cells.

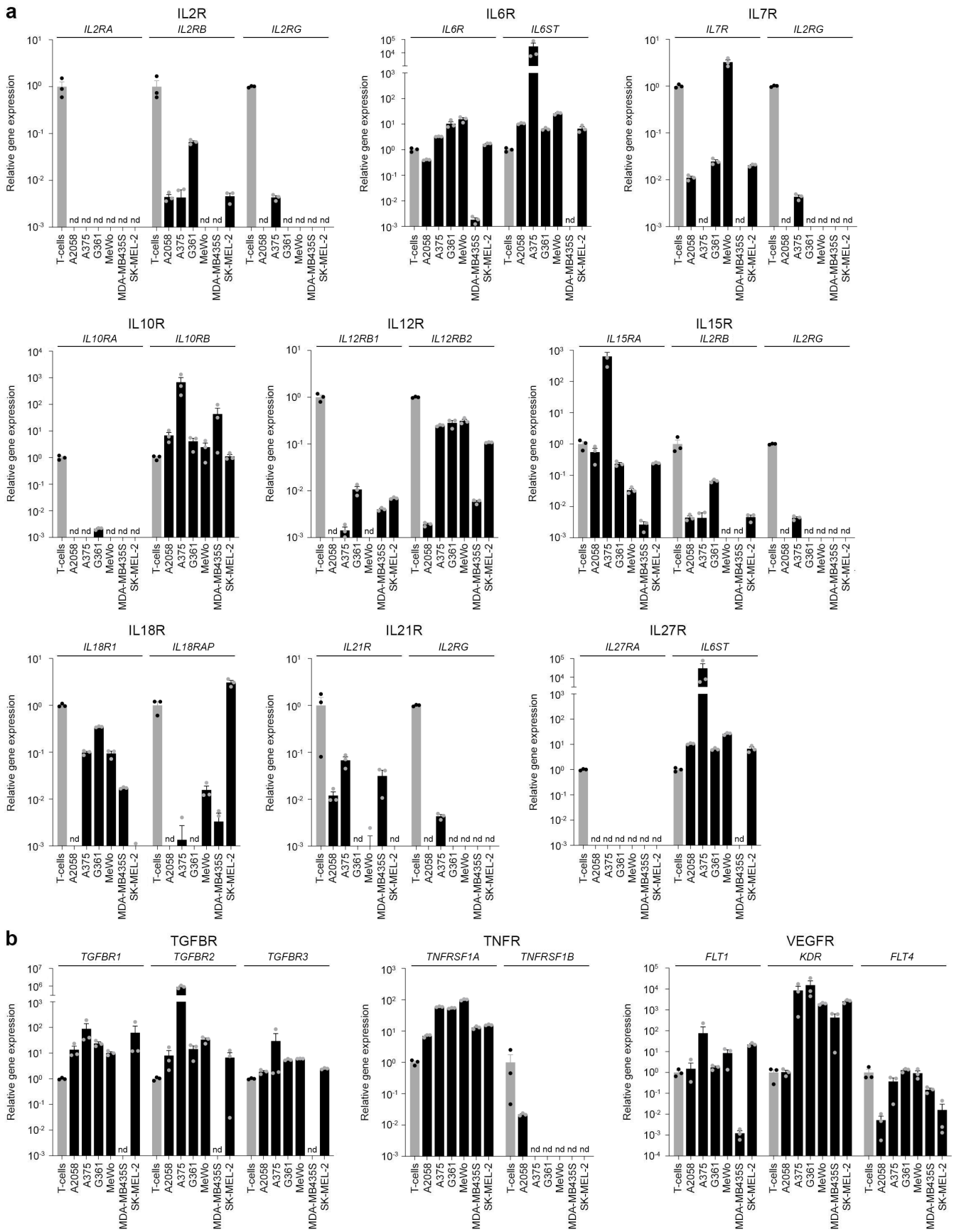
a
IL2R
IL2RA
IL2RB
IL2RG
IL6R
IL6R
IL6ST
IL7R
IL7R
IL2RG
IL10R
IL10RA
IL10RB
IL12R
IL12RB1
IL12RB2
IL15R
IL15RA
IL2RB
IL2RG
IL18R
IL18R1
IL18RAP
IL21R
IL21R
IL2RG
IL27R
IL27RA
IL6ST
Relative gene expression
T-cells
A2058
A375
G361
MeWo
MDA-MB435S
SK-MEL-2
nd
b
TGFBR
TGFBR1
TGFBR2
TGFBR3
TNFR
TNFRSF1A
TNFRSF1B
VEGFR
FLT1
KDR
FLT4

Supplementary Figure 4. Expression of cytokine and growth factor receptors by human melanoma cell lines. Related to Figure 1. Relative gene expression (fold change, mean ± SEM) of **a,** cytokine receptor and **b,** growth factor receptor subunits in human melanoma cell lines (black bars) versus human T-cells (gray bars) as determined by RT-qPCR. Results in (**a**-**b**) represent biologically independent experiments of $n = 3$; nd, not detected as defined by either no amplification or expression level > 1000-fold below the T-cell control. Source data are provided as a Source Data file.

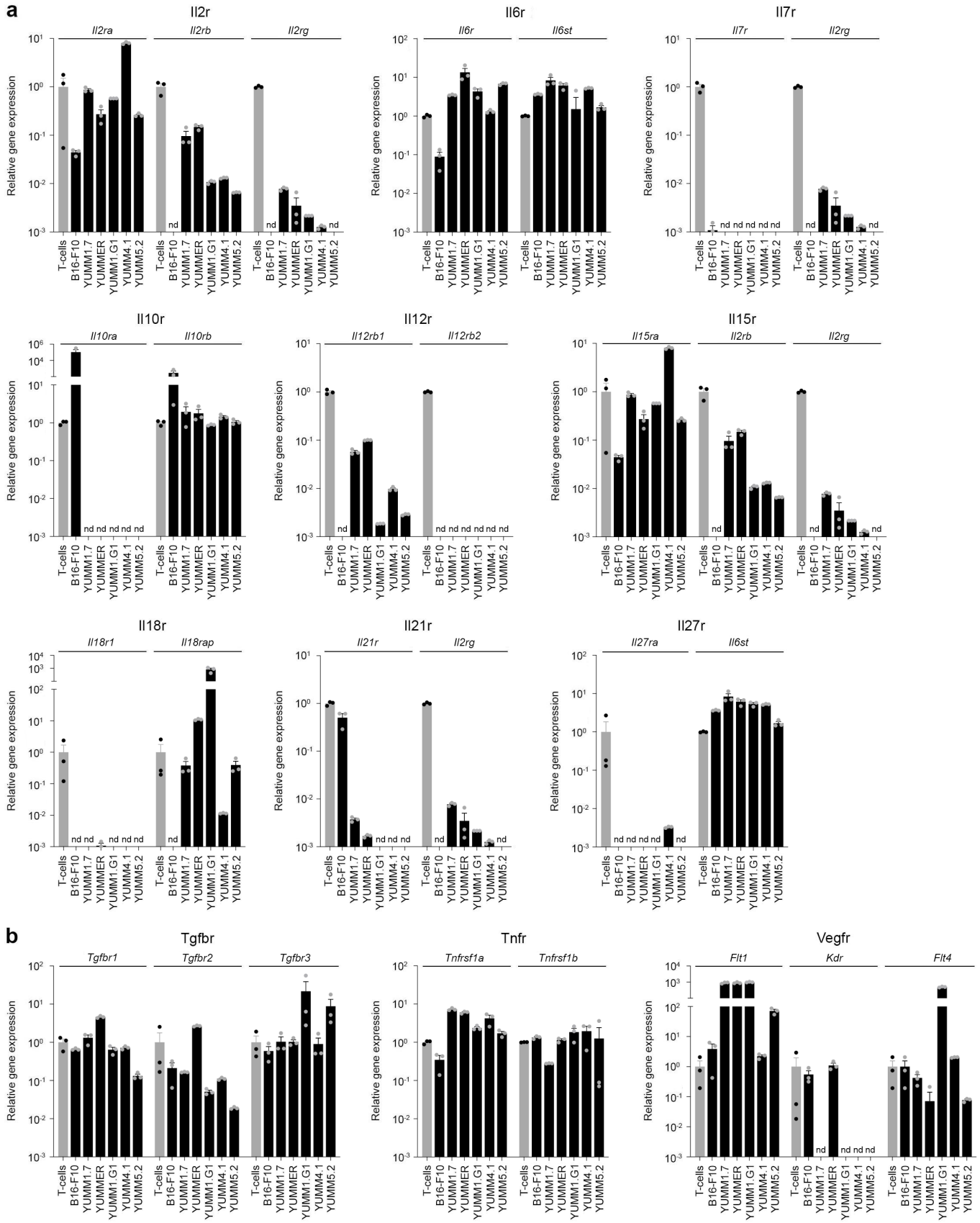
a
Il2r
Il2ra
Il2rb
Il2rg
Il6r
Il6st
Il7r
Il7r
Il2rg
Il10r
Il10ra
Il10rb
Il12r
Il12rb1
Il12rb2
Il15r
Il15ra
Il2rb
Il2rg
Il18r
Il18r1
Il18rap
Il21r
Il21r
Il2rg
Il27r
Il27ra
Il6st
b
Tgfbr
Tgfbr1
Tgfbr2
Tgfbr3
Tnfr
Tnfrsf1a
Tnfrsf1b
Vegfr
Flt1
Kdr
Flt4
Relative gene expression
T-cells
B16-F10
YUMM1.7
YUMMER
YUMM1.G1
YUMM4.1
YUMM5.2
nd

Supplementary Figure 5. Expression of cytokine and growth factor receptors by murine melanoma cell lines. Related to Figure 1. Relative gene expression (fold change, mean ± SEM) of **a,** cytokine receptor and **b,** growth factor receptor subunits in murine melanoma lines (black bars) versus murine T-cells (gray bars) as determined by RT-qPCR. Results in (**a**-**b**) represent biologically independent experiments of n = 3; nd, not detected as defined by either no amplification or expression level > 1000-fold below the T-cell control. Source data are provided as a Source Data file.

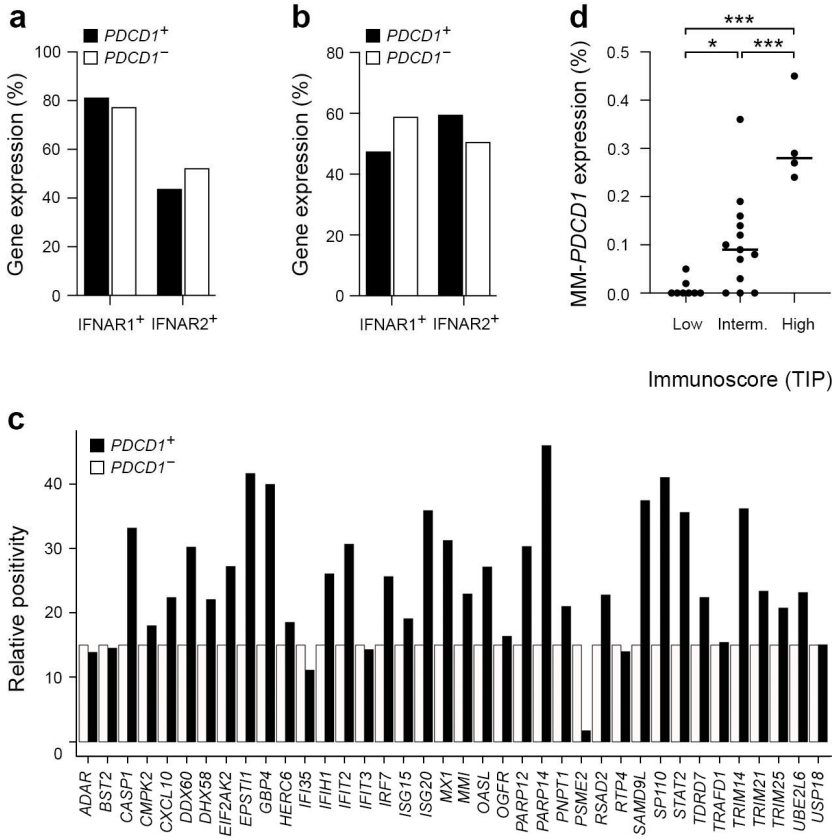

Supplementary Figure 6. Patient *PDCD1*$^+$-melanoma cells co-express type I interferon receptors and are enriched in expression of interferon-stimulated genes (ISGs) and in tumors with high immunoscore. Related to Figure 1. Single-cell RNA-seq analysis of *IFNAR1* or *IFNAR2* positivity in *PDCD1*$^+$ versus *PDCD1*$^-$ patient melanoma cells analyzed from two-independent data sets (**a**[1] , **b**[2]). **c,** Relative positivity of an established ISG signature panel[3] among *PDCD1*$^+$ versus *PDCD1*$^-$ patient melanoma cells as analyzed by single-cell RNA-seq[2]. **d,** Correlation of patient *PDCD1*-expressing tumor cells (bars, median %) with varying immunoscore (low, intermediate, or high) in unsorted patient melanoma tissue lesions with detectable tumor cells, as determined by tumor immunological phenotype (TIP) signature[4] score. Lesional TIP scores were determined by subtracting the summed expression level of established hot genes (*CCL5*, *CD274*, *CD3D*, *CD3E*, *CD3G*, *CD4*, *CD8A*, *CD8B*, *CXCR3*, *CXCR4*, *CXCL9*, *CXCL10*, *CXCL11*, *PDCD1*) versus cold genes (*CXCL1*, *CXCL2*, *CCL20*)[4]. *, $p < 0.05$; ***, $p < 0.001$. Results in (**a-d**) represent data derived from biologically independent samples of (**a**) $n = 1252$ MM cells, (**b-c**) $n = 1 \times 10^4$ MM cells, and (**d**) $n = 8$ (low), $n = 13$ (intermediate), and $n = 4$ (high) tumor lesions. Statistical analyses included (**d**) one-way ANOVA with Tukey post hoc test. Source data, including exact *p*-values, are provided as a Source Data file.

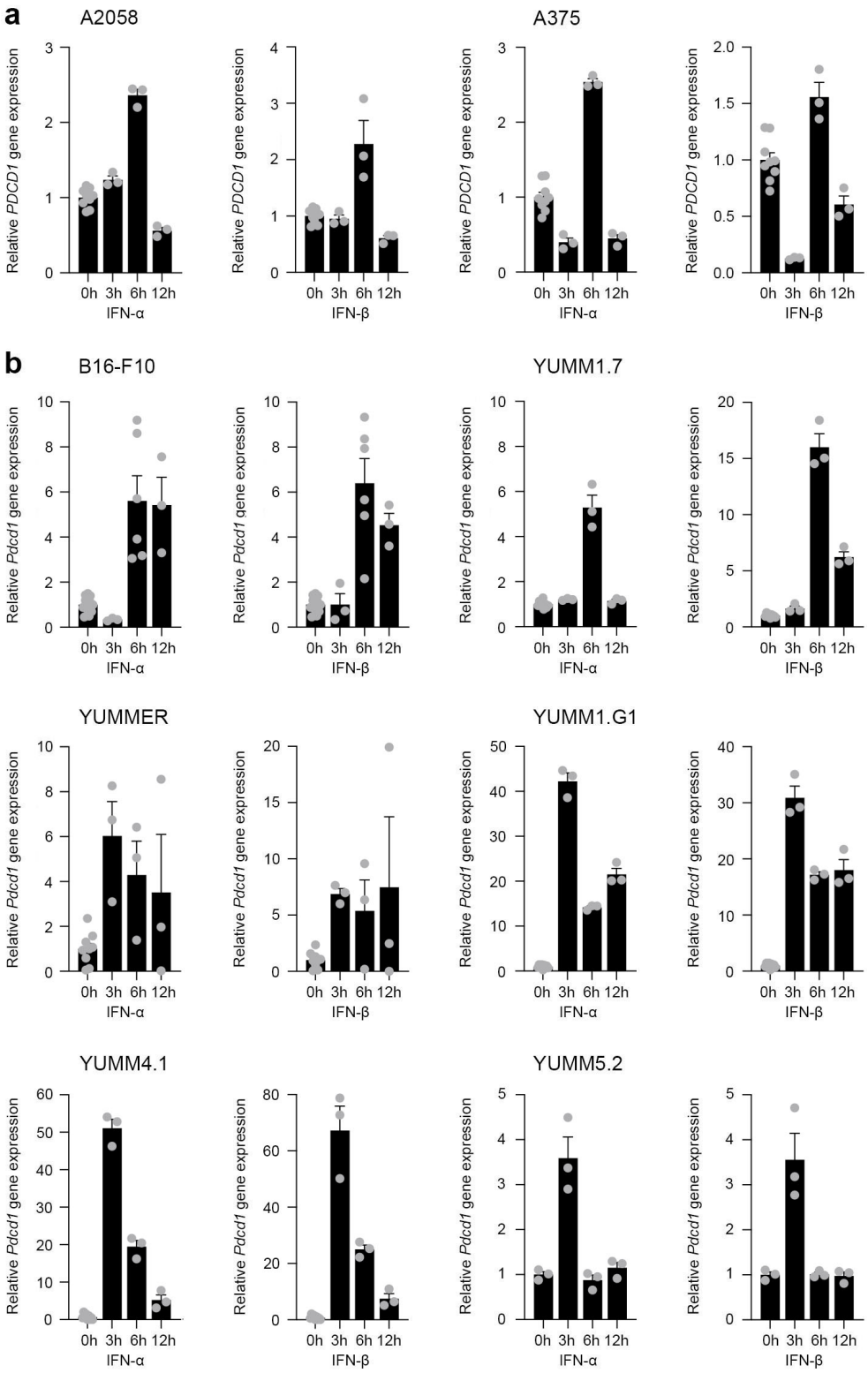

Supplementary Figure 7. Time course of type I interferon cytokine-mediated induction of PD-1 gene expression in melanoma cells. Related to Figure 2. a, Relative *PDCD1* gene expression (fold change, mean ± SEM) in human A2058 or A375 melanoma cells at 0, 3, 6, or 12 hours of treatment with human IFN-α (left) or IFN-β (right). b, Relative *Pdcd1* gene expression (fold change, mean ± SEM) in murine

B16-F10, YUMM1.7, YUMMER, YUMM1.G1, YUMM4.1, or YUMM5.2 melanoma cells at 0, 3, 6, or 12 hours of treatment with mouse IFN-α (left) or IFN-β (right). Results represent biologically independent experiments of **(a)** $n = 9$ (0h), $n = 3$ (3, 6, 12h), **(b)** $n = 12$ (0h), $n = 3$ (3, 12h), $n = 6$ (6h) for B16-F10, $n = 9$ (0h), $n = 3$ (3, 6, 12h) for YUMM1.7, YUMMER, YUMM1.G1, and YUMM4.1, and $n = 3$ (0, 3, 6, 12h) for YUMM5.2 cells. Some data points shown here are also used in Figure 2. Source data are provided as a Source Data file.

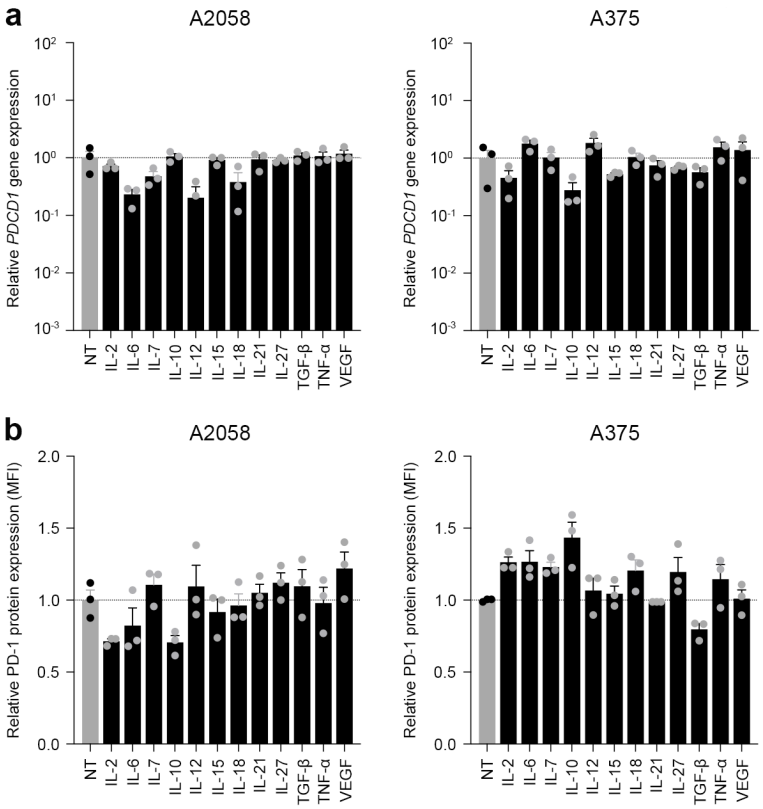

Supplementary Figure 8. Effect of cytokine and growth factor treatment on melanoma cell-PD-1 expression. Related to Figure 2. **a,** Relative *PDCD1* gene (fold change, mean ± SEM) and **b,** PD-1 surface protein (fluorescence intensity, mean ± SEM) expression by human A2058 and A375 melanoma cells treated (black bars) versus not treated (NT, gray bars) with human cytokines or growth factors, as determined by RT-qPCR and flow cytometry, respectively. Results represent biologically independent experiments of (**a**-**b**) $n = 3$. Source data are provided as a Source Data file.

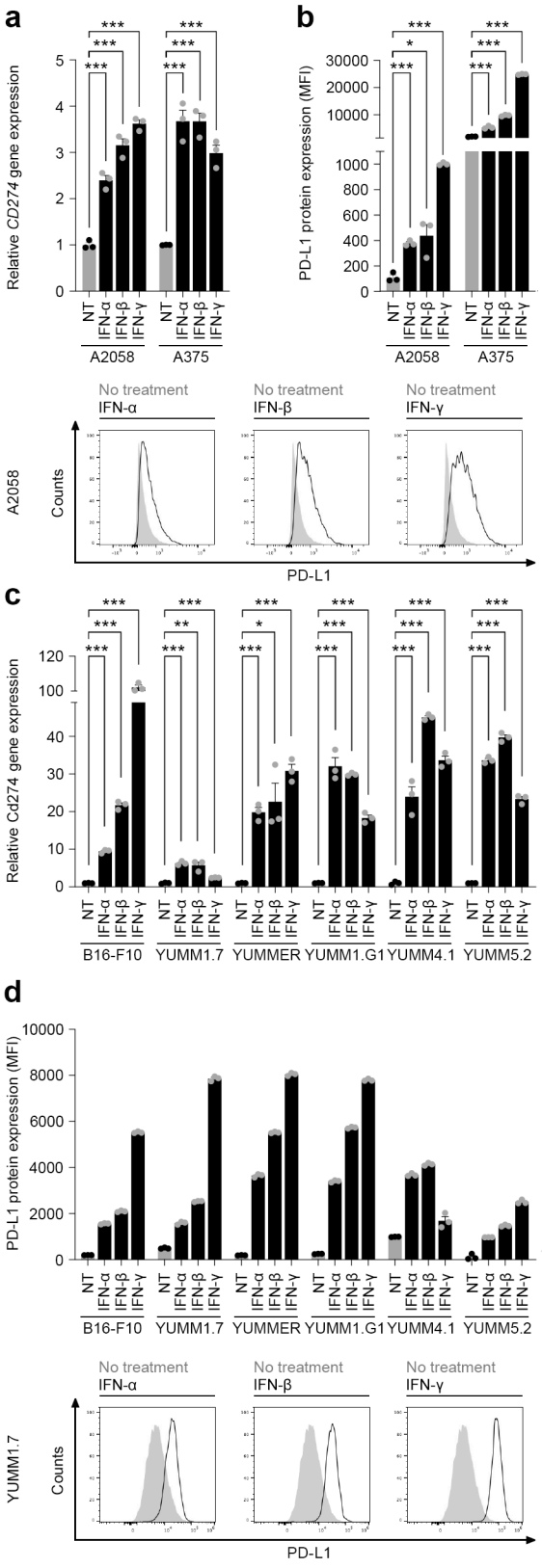

Supplementary Figure 9. Type I and type II interferons induce melanoma cell-intrinsic PD-L1 expression. a, Relative *CD274* (PD-L1) gene (fold change, mean ± SEM) and **b,** PD-L1 surface protein

(fluorescence intensity, mean ± SEM, top) expression by human A2058 and A375 melanoma cells treated (black bars) versus not treated (NT, gray bars) with human type I interferons, IFN-α or IFN-β, or type II interferon, IFN-γ, as determined by RT-qPCR and flow cytometry, respectively. Representative flow cytometric histograms for IFN-α, IFN-β, or IFN-γ treated (unshaded, black lines) versus no treatment control (shaded, gray) A2058 cells are shown (bottom). **c,** Relative *Cd274* (PD-L1) gene (fold change, mean ± SEM) and **d,** PD-L1 surface protein (fluorescence intensity, mean ± SEM) expression by murine melanoma cells treated (black bars) versus not treated (NT, gray bars) with murine IFN-α or IFN-β, or IFN-γ, as determined by RT-qPCR and flow cytometry, respectively. Representative flow cytometric histograms for IFN-α, IFN-β, or IFN-γ treated (unshaded, black lines) versus no treatment control (shaded, gray) YUMM1.7 cells are shown (bottom). Results represent biologically independent experiments of $n = 3$ for **(a-c)** and technical replicates of $n = 3$ for **(d)**. Statistical analyses included the (**a**-**c**) unpaired *t*-test, two-sided. *, $p < 0.05$; **, $p < 0.01$; ***, $p < 0.001$; NS, not significant. Source data are provided as a Source Data file.

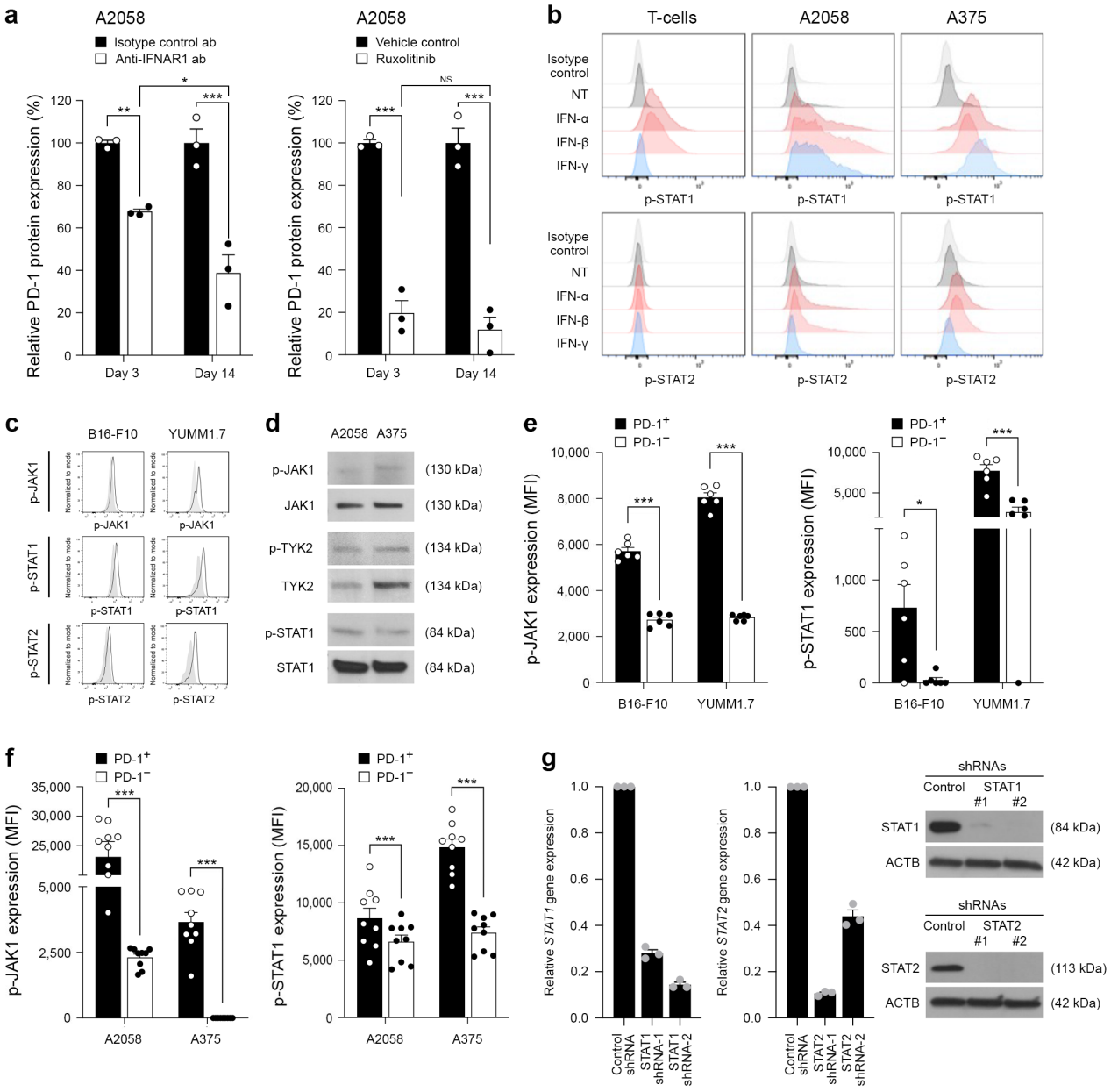

Supplementary Figure 10. Constitutive activation, induction, and extended inhibitor treatment of the melanoma cell-intrinsic type I interferon signaling axis. Related to Figures 2-6. a, Effect of shorter (3 days) versus longer (14 days) durations of continuous treatment with anti-IFNAR1 blocking ab versus isotype control ab (left) or ruxolitinib versus vehicle control (right) on relative PD-1 surface protein expression (percent positivity, mean ± SEM) by human A2058 melanoma cells as determined by flow cytometry. **b,** Relative intracellular levels of phosphorylated (p)-STAT1 (top) and p-STAT2 (bottom) in human melanoma A2058 and A375 cells and human T-cells treated with type I interferons, IFN-α or IFN-β (red histograms), or type II interferon, IFN-γ (blue histograms), versus no treatment (NT, dark gray histograms) or isotype-matched control groups (light gray histograms) as determined by flow cytometry. **c,**

Relative intracellular constitutive levels of p-JAK1, p-STAT1, and p-STAT2 (black histograms) in untreated B16-F10 and YUMM1.7 melanoma cells versus isotype-matched control groups (light gray histograms). **d,** Immunoblot analysis of constitutively expressed p-JAK1, p-TYK2, and p-STAT1 and respective controls in human A2058 and A375 melanoma cells. **e-f,** Expression of p-JAK1 or p-STAT1 in PD-1^+ vs. PD-1^- **e,** murine B16-F10 or YUMM1.7 or **f,** human A2058 or A375 melanoma cells as determined by intracellular FACS analysis. **g,** Stable STAT1 or STAT2 knockdown human A2058 melanoma cell line variants were generated by shRNA-mediated gene silencing using two independent hairpins, shRNA-1 or shRNA-2. STAT1 and STAT2 knockdown compared to respective control shRNA cells was confirmed at both the mRNA (mean ± SEM, left) and protein levels (right) by RT-qPCR and immunoblotting, respectively. Results in (**a**-**f**) represent biologically independent experiments of (**a**) $n = 3$, (**e**) $n = 6$, (**f**) $n = 9$ and (**g**) technical replicates of $n = 3$. Histograms or blots are representative of biologically independent experiments of (**b-d**) $n = 3$, and (**g**) $n = 2$. Statistical analyses included the (**a**) two-way ANOVA with Fisher's LSD post hoc test, and (**e**-**f**) paired *t*-test, two-sided. *, $p < 0.05$; **, $p < 0.01$; ***, $p < 0.001$; NS, not significant. Source data, including exact *p*-values, are provided as a Source Data file.

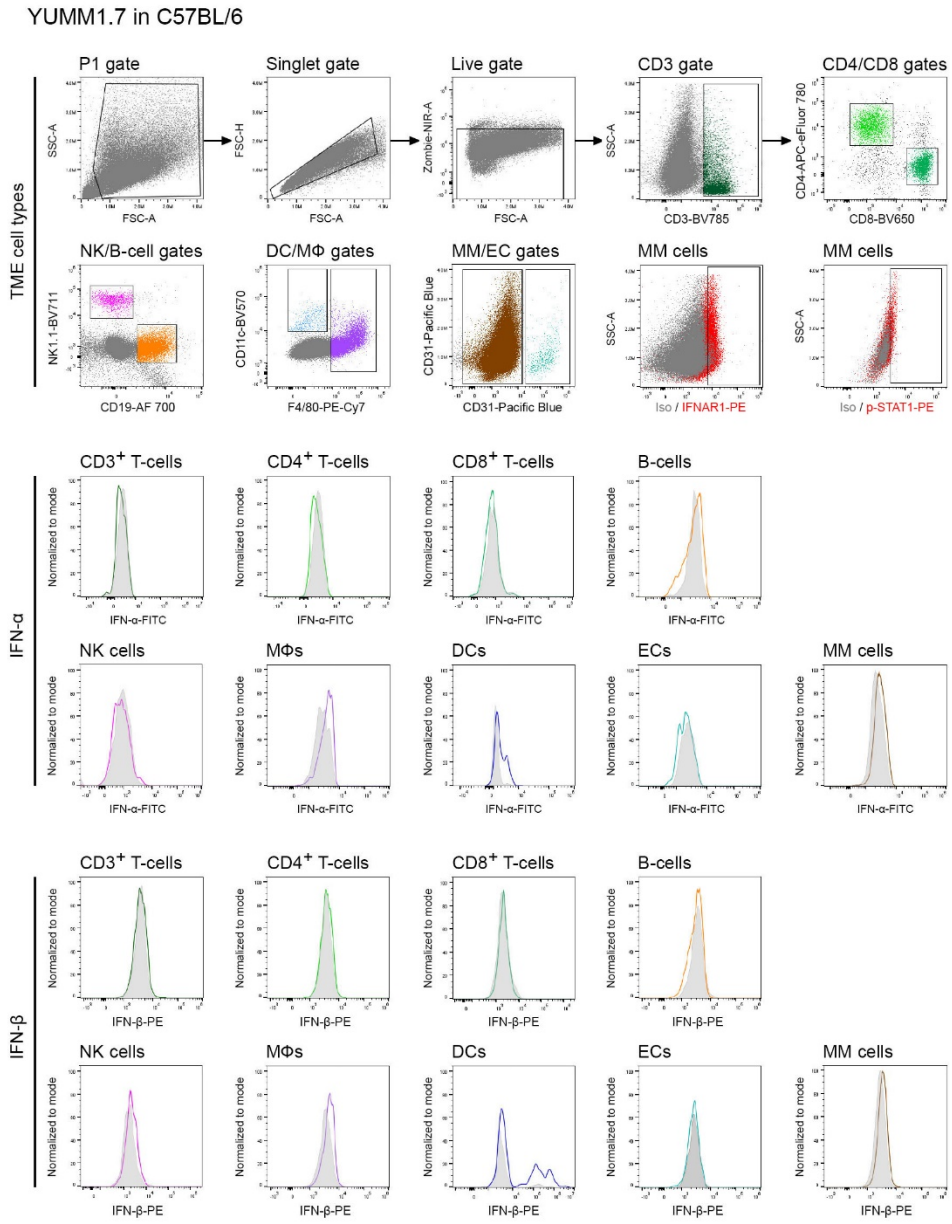

Supplementary Figure 11. Flow cytometry gating strategies for *ex vivo* analysis of type I interferon receptor and cytokine expression by melanoma cells or diverse TME cell types. Related to Supplementary Figures S10, S12. Flow cytometry gating strategies and representative dot plots for analysis of IFN-α, IFN-β, IFNAR1, and p-STAT1 protein expression in TME immune or non-immune cell types of murine YUMM1.7 tumors grown in C57BL/6 mice, including T-cells ($CD3^+$), T-helper cells ($CD3^+CD4^+$), cytotoxic T-cells ($CD3^+CD8^+$), natural killer (NK) cells ($NK1.1^+$), B-cells ($CD19^+$), dendritic cells (DC, $CD11c^+$), macrophages (MΦ, $F4/80^+$), endothelial cells (EC, $CD31^+$), and melanoma (MM) cells ($CD31^-$).

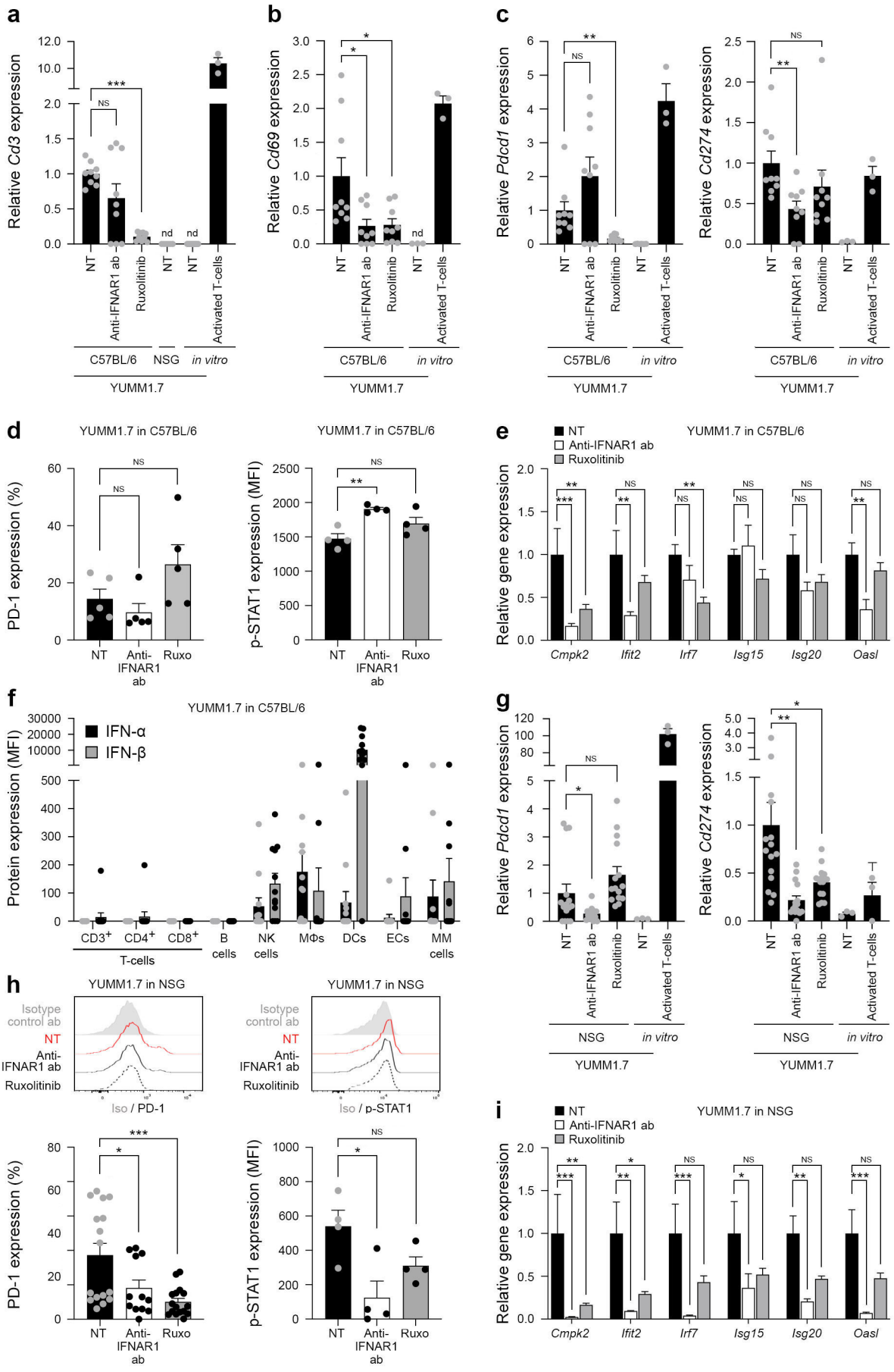
a
Relative Cd3 expression
12.0
10.0
2.0
1.5
1.0
0.5
0.0
***
NS
nd
nd
NT
Anti-IFNAR1 ab
Ruxolitinib
NT
NT
Activated T-cells
C57BL/6
NSG
in vitro
YUMM1.7
b
Relative Cd69 expression
3.0
2.5
2.0
1.5
1.0
0.5
0.0
*
*
nd
NT
Anti-IFNAR1 ab
Ruxolitinib
NT
Activated T-cells
C57BL/6
in vitro
YUMM1.7
c
Relative Pdcd1 expression
6
5
4
3
2
1
0
**
NS
NT
Anti-IFNAR1 ab
Ruxolitinib
NT
Activated T-cells
C57BL/6
in vitro
YUMM1.7
Relative Cd274 expression
2.5
2.0
1.5
1.0
0.5
0.0
NS
**
NT
Anti-IFNAR1 ab
Ruxolitinib
NT
Activated T-cells
C57BL/6
in vitro
YUMM1.7
d
YUMM1.7 in C57BL/6
PD-1 expression (%)
60
40
20
0
NS
NS
NT
Anti-IFNAR1 ab
Ruxo
YUMM1.7 in C57BL/6
p-STAT1 expression (MFI)
2500
2000
1500
1000
500
0
NS
**
NS
NT
Anti-IFNAR1 ab
Ruxo
e
NT
Anti-IFNAR1 ab
Ruxolitinib
YUMM1.7 in C57BL/6
Relative gene expression
2.0
1.5
1.0
0.5
0.0
**
***
NS
**
NS
**
NS
NS
NS
NS
NS
**
Cmpk2
Ifit2
Irf7
Isg15
Isg20
Oasl
f
YUMM1.7 in C57BL/6
Protein expression (MFI)
30000
20000
10000
500
400
300
200
100
0
IFN-α
IFN-β
CD3+
CD4+
CD8+
T-cells
B cells
NK cells
MΦs
DCs
ECs
MM cells
g
Relative Pdcd1 expression
120
100
80
5
4
3
2
1
0
NS
*
NT
Anti-IFNAR1 ab
Ruxolitinib
NT
Activated T-cells
NSG
in vitro
YUMM1.7
Relative Cd274 expression
5.0
4.0
3.0
1.5
1.0
0.5
0.0
*
**
NT
Anti-IFNAR1 ab
Ruxolitinib
NT
Activated T-cells
NSG
in vitro
YUMM1.7
h
YUMM1.7 in NSG
Isotype control ab
NT
Anti-IFNAR1 ab
Ruxolitinib
Iso / PD-1
YUMM1.7 in NSG
Isotype control ab
NT
Anti-IFNAR1 ab
Ruxolitinib
Iso / p-STAT1
PD-1 expression (%)
80
60
40
20
0
***
*
NT
Anti-IFNAR1 ab
Ruxo
p-STAT1 expression (MFI)
1000
800
600
400
200
0
NS
*
NT
Anti-IFNAR1 ab
Ruxo
i
NT
Anti-IFNAR1 ab
Ruxolitinib
YUMM1.7 in NSG
Relative gene expression
2.0
1.5
1.0
0.5
0.0
**
***
*
**
NS
***
NS
*
NS
**
NS
***
Cmpk2
Ifit2
Irf7
Isg15
Isg20
Oasl

Supplementary Figure 12. IFNAR-JAK/STAT axis inhibition suppresses tumor-infiltrating T-cell activation and ISG level and modulates PD-1:PD-L1 expression in murine melanoma grafts. Related to Figures 5 and S11. Relative gene expression (mean ± SEM) of **a,** *Cd3ε,* **b,** *Cd69*, **c,** *Pdcd1* (PD-1, left) and *Cd274* (PD-L1, right), **d,** protein expression of PD-1 (percent positivity ± SEM) and p-STAT1 (fluorescence intensity, mean ± SEM) and **e,** ISG signature gene expression (mean ± SEM) in YUMM1.7 tumors grown in untreated (NT) versus anti-IFNAR blocking ab or ruxolitinib (ruxo) treated C57BL/6 mice, as determined by RT-qPCR or FACS, respectively. Untreated YUMM1.7 cells grown in NSG mice or *in vitro*, as well as activated C57BL/6-derived murine T-cells were used as controls. **f,** Protein expression (fluorescence intensity, mean ± SEM) of IFN-α and IFN-β in diverse TME cell types within YUMM1.7 tumors grown in C57BL/6 mice, as determined by FACS. **g,** Relative gene expression (mean ± SEM) of *Pdcd1* (left) and *Cd274* (right), **h,** protein expression of PD-1 (percent positivity ± SEM, bottom left) and p-STAT1 (fluorescence intensity, mean ± SEM, bottom right), with representative histograms shown (top left and right), and **i,** ISG signature gene expression in YUMM1.7 tumors grown in NSG mice either untreated or treated with anti-IFNAR blocking ab or ruxolitinib as in **a-e**. Results represent biologically independent experiments of (**a**) $n = 9$ (NT, anti-IFNAR1 ab, ruxolitinib; C57BL/6), $n = 15$ (NT; NSG), $n = 6$ (NT; *in vitro*), and $n = 3$ (activated T-cells; *in vitro*), (**b**) $n = 9$ (NT, anti-IFNAR1 ab, ruxolitinib; C57BL/6), $n = 3$ (NT; *in vitro*), and $n = 3$ (activated T-cells; *in vitro*), (**c**, left panel) $n = 9$ (NT, anti-IFNAR1 ab, ruxolitinib; C57BL/6), $n = 6$ (NT; *in vitro*), $n = 3$ (activated T-cells; *in vitro*), (**c**, right panel) $n = 9$ (NT, anti-IFNAR1 ab, ruxolitinib; C57BL/6), $n = 3$ (NT; *in vitro*), $n = 3$ (activated T-cells; *in vitro*), (**d**) $n = 5$ (left panel), $n = 4$ (right panel), (**e**) $n = 9$ (NT), $n = 12$ (anti-IFNAR1 ab), $n = 18$ (ruxolitinib), (**f**) $n = 12$, (**g**) $n = 15$ (NT, anti-IFNAR1 ab, ruxolitinib), $n = 3$ (NT; *in vitro*), $n = 3$ (activated T-cells; in vitro), (**h**, left panel) $n = 16$ (NT) $n = 12$ (anti-IFNAR1 ab), $n = 16$ (ruxolitinib), (**h**, right panel) $n = 4$ (NT, anti-IFNAR1 ab, ruxolitinib), and (**i**) $n = 12$ (NT), $n = 15$ (anti-IFNAR1 ab), and $n = 15$ (ruxolitinib). Statistical analyses included the (**a-c,g**) unpaired t-test, two-sided, (**d,h**) one-way ANOVA with Dunnett post hoc test, and (**e,i**) two-way ANOVA with Dunnett post hoc test. *, $p < 0.05$; **, $p < 0.01$; ***, $p < 0.001$; NS, not significant; nd, not detected. Source data, including exact *p*-values, are provided as a Source Data file.

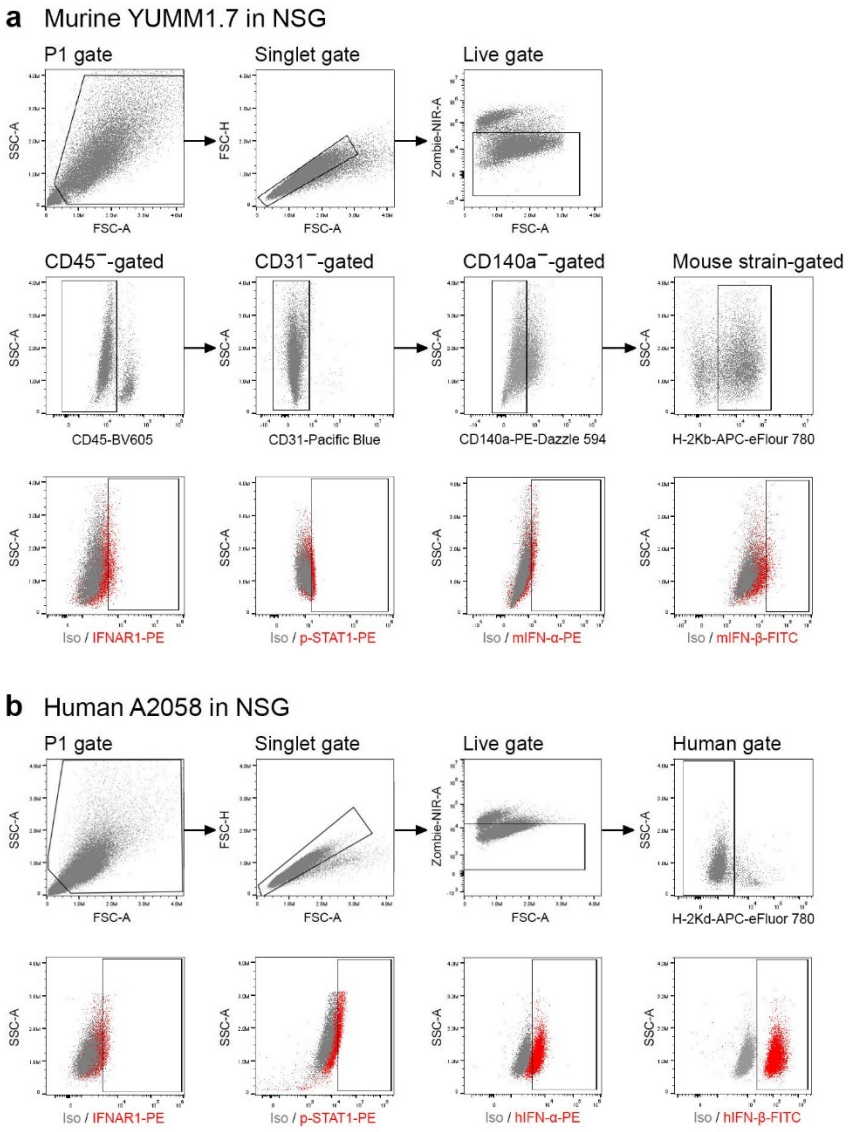

Supplementary Figure 13. Flow cytometry gating strategies for *ex vivo* analysis of tumor-intrinsic type I interferon receptor, cytokine expression, pathway activation in melanoma grafts. Related to Figures S12 and S14. Flow cytometry gating strategies and representative dot plots for **a,** IFNAR1, p-STAT1, mouse (m) IFN-α, or mIFN-β expression by murine YUMM1.7 melanoma cells ($CD45^-CD31^-CD140a^-H\text{-}2Kb^+$) or **b,** IFNAR1, p-STAT1, human (h) IFN-α, or hIFN-β expression by human A2058 melanoma cells ($H\text{-}2Kd^+$) grown in NSG mice.

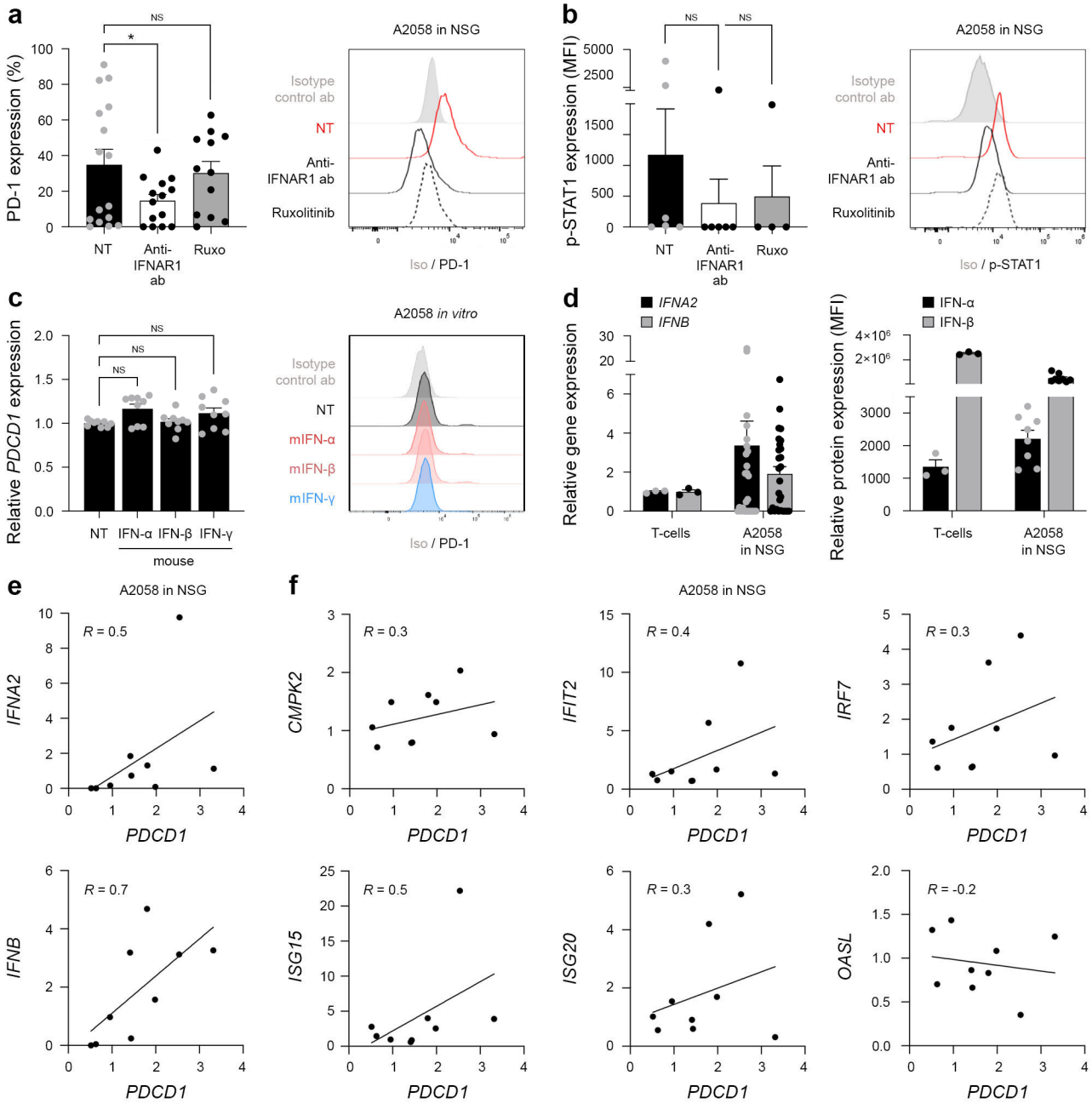

Supplementary Figure 14. IFNAR1 inhibition downregulates human melanoma cell-intrinsic PD-1 expression associated with autocrine type I interferon signaling. Related to Figures 5 and S13. a, Human PD-1 protein (percent positivity, mean ± SEM) and **b,** p-STAT1 (fluorescence intensity, mean ± SEM) expression in A2058 tumors grown in NSG mice either untreated or treated with anti-IFNAR1 blocking ab or ruxolitinib (left), with representative histograms shown (right). **c,** Effect of murine IFN-α, IFN-β, or IFN-γ on PD-1 gene (left, mean ± SEM) or protein (right, representative histograms) expression by A2058 melanoma cell cultures. **d,** Relative gene (left, mean ± SEM) and protein (right, fluorescence intensity, mean ± SEM) expression of human IFN-α or IFN-β by A2058 melanoma xenografts grown in

NSG mice or by T-cell controls. **e,** Correlation of human IFN-α or IFN-β or of **f,** ISG signature gene expresssion with *PDCD1* level in A2058 tumors xenografts in NSG mice. Results represent biologically independent experiments of (**a**) $n = 16$ (NT), $n = 14$ (anti-IFNAR1 ab), $n = 12$ (ruxolitinib), (**b**) $n = 6$ (NT), $n = 6$ (anti-IFNAR1 ab), $n = 4$ (ruxolitinib), (**c**) $n = 9$, (**d**, left panel) $n = 3$ (T-cells), $n = 27$ (A2058; NSG), (**d**, right panel) $n = 3$ (T-cells), $n = 8$ (A2058; NSG), and (**e,f**) $n = 9$. Statistical analyses included (**a**,**b**) one-way ANOVA with Dunnett post hoc test, (**c**) Friedman test with Dunn's post hoc test, and (**e**) Pearson correlation test, two-sided. *, $p < 0.05$; NS, not significant; *R*, Pearson correlation coefficient. Source data, including exact *p*-values, are provided as a Source Data file.

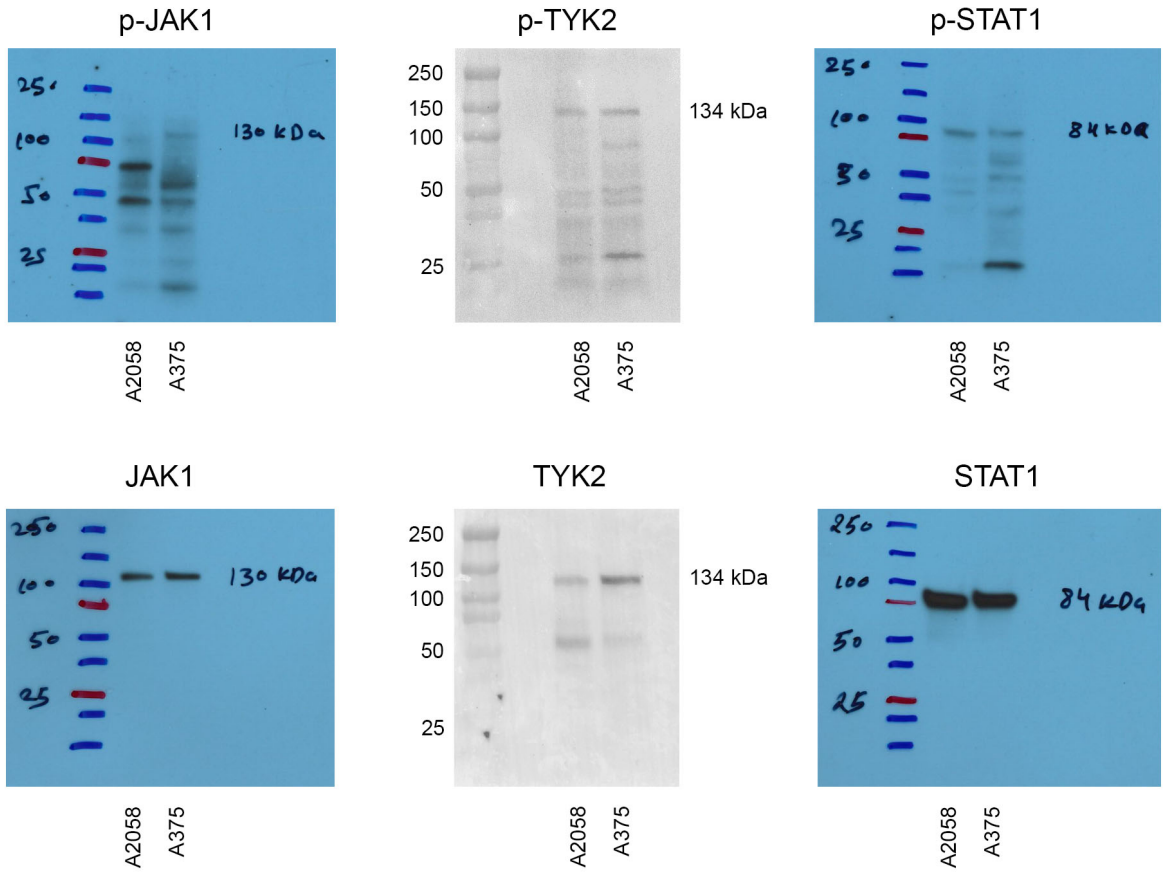

Supplementary Figure 15. Full Western blot film images of constitutively phosphorylated (p)-JAK-1, TYK2, and STAT1 (top) and respective total controls (bottom) in untreated human A2058 and A375 melanoma cells (shown in Figure S10d).

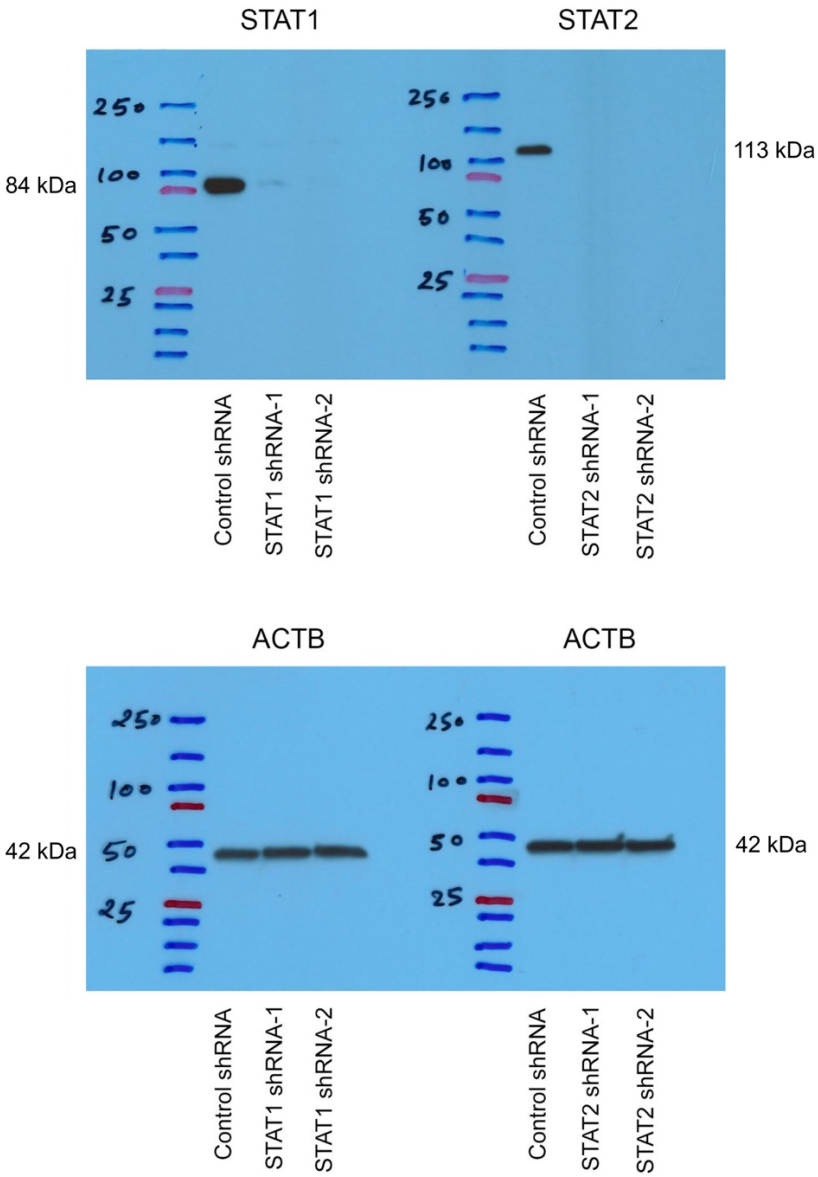

Supplementary Figure 16. Full Western blot film images of total STAT1 (top left) and STAT2 (top right) and respective ACTB controls (bottom) in STAT1 shRNA-1/-2 or STAT2 shRNA-1/-2 vs. corresponding shRNA control human A2058 and A375 melanoma cells (shown in Figure S10g).

Supplementary Tables

Supplementary Table 1 – Human primer sets used for SYBR Green RT-qPCR.

Gene	Forward Primer (5'-3')	Reverse Primer (5'-3')	Annealing Temp (°C)
18srRNA	GATGGGCGGCGGAAAATAG	GCGTGGATTCTGCATAATGGT	68°C
PDCD1	GACAGCGGCACCTACCTCTGTG	GACCCAGACTAGCAGCACCAGG	
PDCD1LG1	TCACTTGGTAATTCTGGGAGC	TTTGAGTTTGTATCTTGGATGCC	
PDCD1LG2	GAGCTGTGGCAAGTCCTCAT	GCAATTCCAGGCTCAACATTA	60°C
IFNGR1	AGTGCTTAGCCTGGTATTCATCTG	GGCTGGTATGACGTGATGAGTG	
IFNGR2	CTCCATTCTGCCTGGGTGACAA	CGTGGAGGTATCAGCGATGTCA	
IFNAR1	CGCCTGTGATCCAGGATTATCC	TGGTGTGTGCTCTGGCTTTCAC	
IFNAR2	ACCGTCCTAGAAGGATTCAGCG	CCAACAATCTCAAACTCTGGTGG	
IL2RA	GAGACTTCCTGCCTCGTCACAA	GATCAGCAGGAAAACACAGCCG	
IL2RB	GGTGGAACCAAACCTGTGAGCT	GGTGACGATGTCAACTGTGGTC	
IL2Rg	CACTCTGTGGAAGTGCTCAGCA	GAGCCAACAGAGATAACCACGG	
IL6Ra	GACTGTGCACTTGCTGGTGGAT	ACTTCCTCACCAAGAGCACAGC	
IL6ST	CACCCTGTATCACAGACTGGCA	TTCAGGGCTTCCTGGTCCATCA	
IL7Ra	ATCGCAGCACTCACTGACCTGT	TCAGGCACTTTACCTCCACGAG	
IL10RA	GCCGAAAGAAGCTACCCAGTGT	GGTCCAAGTTCTTCAGCTCTGG	
IL10RB	GGAATGGAGTGAGCCTGTCTGT	AAACGCACCACAGCAAGGCGAA	
IL12RB1	TGAGATTCTCGGTGGAGCAGCT	CTGTAGTCGGTAAGTGACCTCC	
IL12RB2	AGACCTCAGTGGTGTAGCAGAG	TGATGACCAGCGGTTCAGGATC	
IL15RA	TGGCTATCTCCACGTCCACTGT	CATGGCTTCCATTTCAACGCTGG	
IL18R1	GGAGGCACAGACACCAAAAGCT	AGGCACACTACTGCCACCAAGA	
IL18RAP	GCACAAAGTCCAGCGGTAACCT	GTCCACGAACTCACAGTATCCG	
IL21RA	ACCAGTCTGGCAACTACTCCCA	AGGGTCTTCGTAATCTGAGCGC	
IL27RA	GTGTGGGTATCAGGGAACCTCT	TCCTTCTGGACTCAGCTCACGA	
TGFBR1	GACAACGTCAGGTTCTGGCTCA	CCGCCACTTTCCTCTCCAAACT	
TGFBR2	GTCTGTGGATGACCTGGCTAAC	GACATCGGTCTGCTTGAAGGAC	
TGBR3	TGGAGTCTCCTCTGAATGGCTG	CCATTATCACCTGACTCCAGATC	
TNFRSF1A	CCGCTTCAGAAAACCACCTCAG	ATGCCGGTACTGGTTCTTCCTG	
TNFRSF1B	CGTTCTCCAACACGACTTCATCC	ACGTGCAGACTGCATCCATGCT	
FLT1	CCTGCAAGATTCAGGCACCTATG	GTTTCGCAGGAGGTATGGTGCT	
KDR	GGAACCTCACTATCCGCAGAGT	CCAAGTTCGTCTTTTCCTGGGC	
FLT4	TGCGAATACCTGTCCTACGATGC	CTTGTGGATGCCGAAAGCGGAG	
STAT1	ATGGCAGTCTGGCGGCTGAATT	CCAAACCAGGCTGGCACAATTG	
STAT2	CAGGTCACAGAGTTGCTACAGC	CGGTGAACTTGCTGCCAGTCTT	

Supplementary Table 2 - Human primer sets used for TaqMan qPCR.

Gene	Resource	Assay ID	5'-Dye/3'-Quencher	Annealing Temp (°C)
ACTB	Thermo Fisher Scientific (Cat# 4331182)	Hs01060665_g1	FAM/MGB	60ºC
IFNA2		Hs00265051_s1		
IFNB		Hs01077958_s1		
ISG15		Hs01921425_s1		
ISG20		Hs00158122_m1		
OASL		Hs00984387_m1		
IFIT2		Hs01922738_s1		
IRF7		Hs01014809_g1		
CMPK2		Hs01013364_m1		

Supplementary Table 3 – Murine primer sets used for SYBR Green RT-qPCR.

Gene	Forward Primer (5'-3')	Reverse Primer (5'-3')	Annealing Temp (°C)
Actb	CATCGTACTCCTGCTTGCTG	AGCGCAAGTACTCTGTGTGG	58°C
Pdcd1	CGGTTTCAAGGCATGGTCATTGG	TCAGAGTGTCGTCCTTGCTTCC	68°C
Pdcd1lg1	TGCGGACTACAAGCGAATCACG	CTCAGCTTCTGGATAACCCTCG	58°C
Pdcd1lg2	ACTTCAGCTGCATGTTCTGG	GGGTTCCATCCGACTCAGAG	60°C
Ifngr1	CTTGAACCCTGTCGTATGCTGG	TTGGTGCAGGAATCAGTCCAGG	
Ifngr2	CCTTCCAGCAATGACCCAAGAC	TGTGATGTCCGTACAGTTCGGC	
Ifnar1	CCAAGGCAAGAGCTATGTCCTG	CAGTGCGTAGTCTGGACATTTGC	
Ifnar2	GAGCCTAGAGACTATCACACCG	TACCAGAGGGTGTAGTTAGCGG	
Il2ra	GCGTTGCTTAGGAAACTCCTGG	GCATAGACTGTGTTGGCTTCTGC	
Il2rb	CTCAAGTGCCACATCCCAGATC	AGCACTTCCAGCGGAGAGATCT	
Il2rg	GGAGCAACAGAGATCGAAGCTG	CCACAGATTGGGTTATAGCGGC	
Il6ra	TGCAGTTCCAGCTTCGATACCG	TGCTTCACTCCTCGCAAGGCAT	
Il6st	CTCTGAGTCCTTGAAGGCGTAC	CCATTCTGGTCGTCCACAGGAA	
Il7ra	CACAGCCAGTTGGAAGTGGATG	GGCATTTCACTCGTAAAAGAGCC	
Il10ra	CCAAACCAGTCTGAGAGCACCT	CAGGACAATGCCTGAGCCTTTC	
Il10rb2	CTGTGAACGGACAGGCAATGAC	ATGAGCCACAGCACGACAAAGC	
Il12rb1	GGACTGGAATGTGTCTGAAGAGG	CCACGAATGTCACCAAGCACAC	
Il12rb2	TTGGACGGCATCAGTGTCTGCA	TCCGACTTTGCAGAGACCTGGT	
Il15ra	GACACCAAAGGTGACCTCACAG	CTGTCTCTGTGGTCATTGCGGT	
Il18r1	AGAGCTGATCCAGGACACATGG	TGGTGGACAGAAAACACGCAGG	
Il18rap	ACAACACGGACCATACGGCTGA	GTACCAGTAGAGGAAAGCAGCTG	
Il21ra	CACTGACTACCTCTGGACCATC	GCAGAAGGTCTCTTGGTCCTGA	
Il27ra	CCAACCTGTCTCTGGTGTGCTT	TACTCCAACGGTTTCCTGGTCC	
Tgfbr1	TGCTCCAAACCACAGAGTAGGC	CCCAGAACACTAAGCCCATTGC	
Tgfbr2	CCTACTCTGTCTGTGGATGACC	GACATCCGTCTGCTTGAACGAC	
Tgfbr3	TCTCCGCTGAATGGCTGTGGTA	CCGACTCCAAATCTTCGTAGCC	
Tnfrsf1a	GTGTGGCTGTAAGGAGAACCAG	CACACGGTGTTCTGAGTCTCCT	
Tnfrsf1b	TGACAGGAAGGCTCAGATGTGC	ATGCTTGCCTCACAGTCCGCAC	
Flt1	TGGATGAGCAGTGTGAACGGCT	GCCAAATGCAGAGGCTTGAACG	
Kdr	CGAGACCATTGAAGTGACTTGCC	TTCCTCACCCTGCGGATAGTCA	
Flt4	AGACTGGAAGGAGGTGACCACT	CTGACACATTGGCATCCTGGATC	
Cd69	GGGCTGTGTTAATAGTGGTCCTC	CTTGCAGGTAGCAACATGGTGG	

Supplementary Table 4 - Murine primer sets used for TaqMan qPCR.

Gene	Resource	Assay ID	5'-Dye/3'-Quencher	Annealing Temp (°C)
Actb	Thermo Fisher Scientific (Cat# 4331182)	Mm00607939_s1	FAM/MGB	60ºC
Ifna2		Mm00833961_s1		
Ifnb1		Mm00439552_s1		
Isg15		Mm01705338_s1		
Isg20		Mm00469585_m1		
Oasl1		Mm00455081_m1		
Ifit2		Mm00492606_m1		
Irf7		Mm00516793_g1		
Cmpk2		Mm00469582_m1		
Cd3e		Mm01179194_m1		

Supplementary References

1 Tirosh, I. *et al.* Dissecting the multicellular ecosystem of metastatic melanoma by single-cell RNA-seq. *Science* **352**, 189-196 (2016). https://doi.org:10.1126/science.aad0501

2 Biermann, J. *et al.* Dissecting the treatment-naive ecosystem of human melanoma brain metastasis. *Cell* **185**, 2591-2608 e2530 (2022). https://doi.org:10.1016/j.cell.2022.06.007

3 Liu, H. *et al.* Tumor-derived IFN triggers chronic pathway agonism and sensitivity to ADAR loss. *Nat Med* **25**, 95-102 (2019). https://doi.org:10.1038/s41591-018-0302-5

4 Wang, H. *et al.* Tumor immunological phenotype signature-based high-throughput screening for the discovery of combination immunotherapy compounds. *Sci Adv* **7** (2021). https://doi.org:10.1126/sciadv.abd7851